SEA ICE RETRIEVALS FROM WINDSAT DATA

Guoqing Lin
Computational Physics, Inc.
Springfield, VA, USA
Email: gary.lin@nrl.navy.mil

Li Li and Peter W. Gaiser
Remote Sensing Division
Naval Research Laboratory
Washington, DC, USA

***Abstract* – This paper presents sea ice environmental parameter retrieval algorithms using data from WindSat, a fully polarimetric passive microwave radiometer. Sea ice concentration and age are retrieved from WindSat data by adapting NASA-TEAM (NT) algorithm, which has been operationally used for Special Sensor Microwave/Imager (SSM/I). The tie-points and weather filters are modified. The modified NT algorithm includes sea ice climatology and land contaminations. We develop an alternative algorithm to retrieve snow-layered sea ice in the Southern Hemisphere as a proxy to the enhanced NT (NT2) algorithm. We also develop algorithms using WindSat 10.7 GHz channels. Preliminary results show that modified NT and proxy NT2 algorithms work compatibly well with NT and NT2 algorithms, respectively.**

Keywords: sea ice, WindSat, algorithm, NASA-TEAM.

I. INTRODUCTION

WindSat is a risk reduction demonstration project for the National Polar-orbiting Operational Environmental Satellite System (NPOESS) Conically-scanned Microwave Imager Sounder (CMIS) instrument. Besides its primary goal of demonstrating the capability to remotely sense the ocean surface wind vector [1], WindSat also provides data for retrievals of other environmental data records (EDRs) such as land EDRs and sea ice EDRs. In this paper, we present the sea ice EDR retrieval algorithms using WindSat data.

Sea ice covers about 10% of the world oceans. Monitoring and studying of sea ice, its coverage, change and trend are important in science, military and commerce [2-4]. Passive microwave satellite monitoring and observations of sea ice began in 1972 by an Electrically Scanning Microwave Radiometer (ESMR) aboard NASA Nimbus 5 satellite. The Scanning Multi-channel Microwave Radiometer (SMMR) and later the Special Sensor Microwave/Imager (SSM/I) have been providing operational sea ice observations for the past quarter century. SSM/I, and its follow-on SSMI/S (Special Sensor Microwave Imager/Sounder), will continue operation in the next few years and then be replaced by the new NPOESS/CMIS instrument with new capabilities. WindSat provides a bridge between SSM/I and CMIS. It shares channels with SSM/I at 18.7, 23.8 and 37 GHz and adds 10.7 and 6.8 GHz channels, but lacks the 85 GHz that SSM/I has. The operational NASA-TEAM (NT) algorithm uses the shared channels to retrieve sea ice concentration and age [5], while the enhanced NT (NT2) algorithm also uses 85 GHz channels from SSM/I to retrieve snow-layered sea ice concentrations [6]. These algorithms are adapted to process WindSat data. In Section II we identify possible sea ice regions and quantify land contaminations. In Section III we describe the NT algorithm adaptation and modification. We also describe the proxy NT2 algorithm and algorithms using 10 GHz channels. Section IV shows the preliminary results. Section V concludes this paper with some discussions.

II. SEA ICE CLIMATOLOGY AND LAND CONTAMINATION

A. Sea Ice Extent Climatology

The possible sea ice regions are defined by using historical sea ice data retrieved from SMMR and SSM/I [7-8] from 1978 to 2003. These datasets are used to obtain climatologically maximum sea ice extent for every calendar month. The lines of maximum sea ice extent are obtained at 5-degree longitude increments at about 30% ice concentration. A 2- to 3-degree latitude margin is added in the equator direction. These lines are visually inspected and some manual adjustment is applied. Fig. 1 shows two examples in the Southern Hemisphere. The resulting monthly ice extent lines are used to confine possible sea ice regions within the red lines in Fig. 2 and the areas outside are defined as climatologically ice free. Such confinement reduces the spurious sea ice retrievals in open oceans, which often appear in daily nowcast [9] and cumulatively show outside the red lines in Fig. 2.

B. Contamination from Land and Permanent Snow and Ice

Since all WindSat channels at 6.8, 10.7, 18.7, 23.8, and 37 GHz have been beam averaged to the largest common footprint at 6.8 GHz channels [1], which is about 40 x 60 km at half power beam width, many WindSat pixels contain

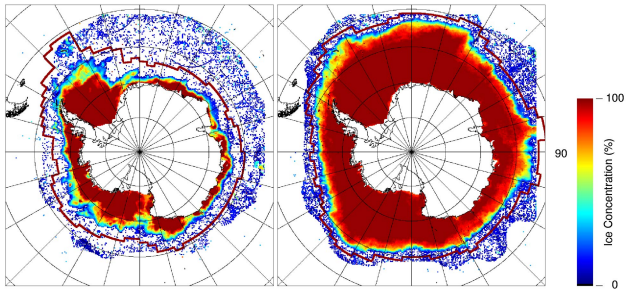

a). February b). October

Fig. 1. The envelopes (red lines) of the climatologically maximum sea ice extent in the Southern Hemisphere in a) February and b) October, along with maximum sea ice concentration retrieved from SMMR and SSM/I data using both BOOTSTRAP and NASA TEAM algorithms.

mixture of different surface types. One surface type may be regarded as contamination to others, since different materials are distinctively different in emissivities [10]. Contamination to the open water, including possible sea ice regions, from other surface types is quantified by convolving WindSat antenna pattern at 6.8 GHz within 200 km diameter with 1-km resolution land-cover databases by the University of Maryland [11] and by the U.S. Geological Survey [12]. These two databases are combined in a conservative manner, taking non-water pixels from either database to compute land and/or permanent snow/ice contamination to water. The values are pre-computed and saved as look-up tables in discrete geo-locations and footprint compass azimuth angles. The quantified contamination identifies the false sea ice retrievals in the coastal areas that often appear in daily nowcast [9].

III. Sea Ice Algorithm Adaptation and Re-development

A. Adaptation and Modification of NASA-TEAM Algorithm

Many sea ice retrieval algorithms have been developed to process SSM/I data [2,7-9]. We adapt the NASA-TEAM (NT) algorithm [5] to process WindSat data. The basic assumptions of the algorithm may be expressed as:

$$T = T_A C_A + T_B C_B + T_W C_W, \quad (1)$$

$$C_A + C_B + C_W = 1, \quad (2)$$

where T is the brightness temperature (TB), C is the sea ice concentration, and the subscripts A, B and W represent three sea ice types: Types A and B in the Antarctic region (first-year (FY) and multi-year (MY) in the Arctic region) and open water, respectively. The equations may be solved by using spectral gradient ratio, G(37v19v), between 37 and 18.7 GHz vertical polarizations and the spectral polarization ratio, P(19v19h), between 18.7 GHz V-pol and H-pol as the following

$$C_A = (A_0 + A_1 P + A_2 G + A_3 PG) / D, \quad (3)$$

$$C_B = (B_0 + B_1 P + B_2 G + B_3 PG) / D, \quad (4)$$

where $D = D_0 + D_1 P + D_2 G + D_3 PG$,

$$P_{19v19h} = \frac{T_{18.7v} - T_{18.7h}}{T_{18.7v} + T_{18.7h}}, \quad G_{37v19v} = \frac{T_{37v} - T_{18.7v}}{T_{37v} + T_{18.7v}},$$

and coefficients A_i, B_i and D_i (i = 1,3) are determined using tie-point TBs over pure Type A, B and W scenes [13].

The NT algorithm employs two weather filters: one with static threshold value of G(37v19v) [13] and another with static threshold value of G(23v19v) [14]. These filters reduce the majority of false sea ice retrievals in open waters. However, spurious false sea ice retrievals still appear in daily nowcast [9]. One way to reduce the weather effects is to confine the possible sea ice regions in climatological areas, as described in Section II.A. An additional way is to use dynamic threshold values of G(37v19v) and G(23v19v), which we describe below.

B. Modified NT Algorithm with Dynamic Weather Filter Set

The TBs from different channels are not completely independent of each other. We modify the static weather filters used in NT algorithm by relating threshold G(37v19v) and G(23v19v) values to P(19v19h), coupled with relating threshold G(37v19v) values to G(23v19v). Such a filter set is derived using a statistical approach. Fig. 2 shows joint probability density functions (JPDFs) and a filter component in the P(19v19h) - G(37v19v) space. Fig. 2a shows the JPDF from WindSat data collected in the last three years in the Northern possible sea ice region without contamination from land or permanent snow and ice as described in Section II. Fig. 2b shows the JPDF in the south, and Fig. 2c shows the JPDF in two 5-degree zones south of northern possible sea ice region boundary and north of southern boundary. Fig. 2c serves as a statistical reference of P(19v19h) - G(37v19v) distribution in open waters close to the possible sea ice regions. Fig. 2c and the JPDF in the Equator region (figure not shown here but extends lower) demonstrate the need of confining the sea ice retrievable measurements to the climatologically possible sea ice regions in reducing the sporadic false sea ice retrievals in the open waters. The dynamic weather filter set consists of three parts: (1) excluding "open water" points when they fall above the blue dash lines in Fig. 2 or (logical "or") Fig. 3 or to the right of the blue dash lines in Fig. 4; (2) identifying "sea ice retrievable" points when they fall below the red solid lines in Fig. 2 and (logical "and") Fig. 3 and to the left of the red solid lines in Fig. 4; and (3) buffering a small fraction of "undetermined" points in between.

Fig. 3 shows the JPDF in the P(19v19h) - G(23v19v) space in the northern and southern possible sea ice regions. The filter lines are determined in a similar manner as in Fig. 2.

Fig. 4a shows the JPDF in the G(37v19v) - G(23v19v) space. When the neighboring 3 x 3 points are available (in most cases), edge enhanced G values are used as shown in Fig. 4b, which gives clearer sea ice edge (Fig. 4c vs 4d) and extends the edge a few pixels to the "open water" side. Sobel finite impulse response kernels in the along-scan and cross-scan directions are used for edge enhancement [15].

Also shown in Fig. 2 are the NT algorithm triangles in blue solid lines. The tie-point TBs at vertices "A" and "B" ("FY" and "MY" in Fig 2a) are determined by matching P(19v19h) - G(37v19v) values from SSM/I data with WindSat data. The tie-point TBs for vertex "W" is determined by the low 25 percentile of the minimum TBs from each WindSat orbit in the last three years. We call this algorithm "WindSat MNT" algorithm.

C. WindSat Proxy NT2 Algorithm

Fig. 2b shows a pronounced ridge between the A-W and A-B lines. The ridge closely resembles the snow-layered "Type C" sea ice described in the enhanced NT (NT2) algorithm [6]. Based on this feature, we develop WindSat

proxy NT2 algorithm for the southern hemisphere. This algorithm uses the same weather filter set as the MNT algorithm and the same tie-point at "W". The tie-point for the proxy "Type C" is determined visually along the ridge. The tie-point for "Type A' " is chosen at the maximum JPD value near "A". The algorithm triangle is shown in Fig. 2b in blue dot lines. We call this algorithm "WindSat PNT2" algorithm.

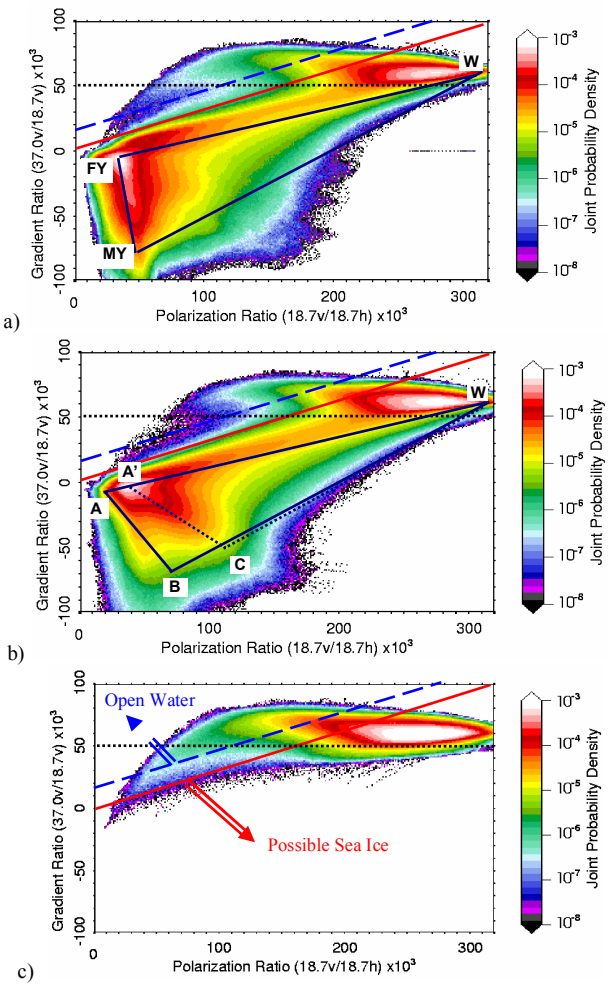

Fig. 2. JPDFs in P(19v19h) - G(37v19v) space in a) the northern climatologically possible sea ice region, b) the southern region and c) 5-degree zones adjacent to the N. and S. boundaries. The modified weather filter is shown in red solid lines. Black dot line is the filter used in the original NT algorithm. Also shown in the figures are the algorithm triangles. All triangle sides are in the form of $y = y_0 + s/(x-x_0)$.

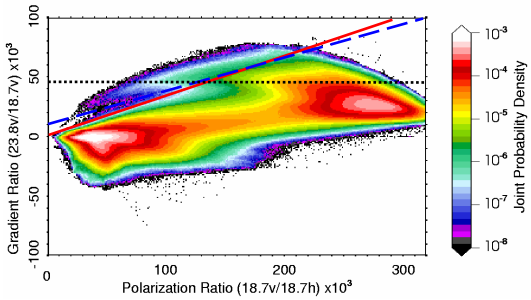

Fig. 3. JPDF in the P(19v19h) - G(23v19v) space measured in the northern and southern climatologically possible sea ice regions. The modified weather filter is shown in red solid line. The black dot line is the original NT filter.

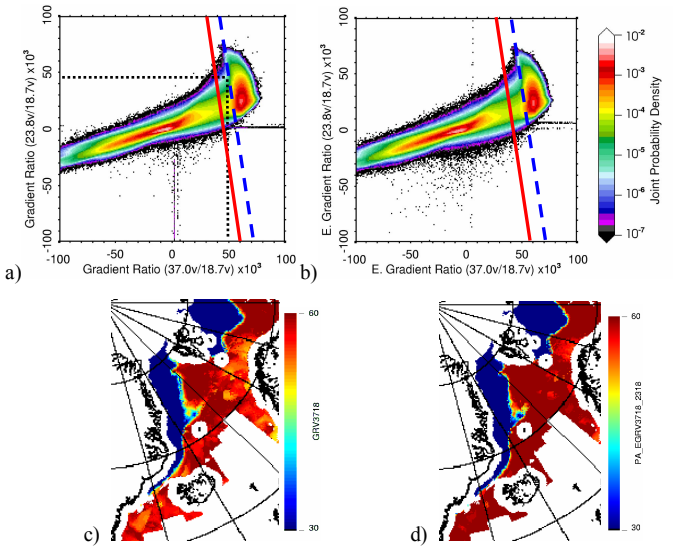

Fig. 4. a) JPDF and b) enhanced JPDF in G(37v19v) - G(23v19v) space in the northern and southern possible sea ice regions. The modified weather filter is shown in red solid lines. Black dot lines are the original NT algorithm filters. c) shows the sea ice edge by G(37v19v) field, while d) shows the edge in the principal axis of the enhanced gradient ratio pair EG(37v19v)-EG(23v19v).

D. Algorithms using WindSat 10.7 GHz Channels

We make use of the additional WindSat channels at 10.7 GHz. The algorithm triangles and weather filter set are developed similar to WindSat MNT and PNT2 algorithms. The filter set makes use of JPDFs in a combination of polarization ratios and gradient ratios (enhance gradient ratios when available) from 10.7 GHz and above. We call them MNT10 for the north and south hemisphere and PNT10 for the south hemisphere. The algorithms for the southern hemisphere are shown in Fig. 5.

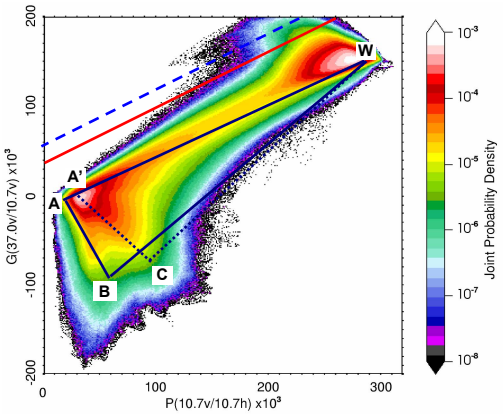

Fig. 5. JPDF in P(10v10h)-G(37v10v) space in the southern hemisphere. 10 GHz NT algorithm triangle is shown in solid lines, while the proxy NT2 algorithm is in dot lines. All triangle sides are in the form of $y = y_0 + s/(x-x_0)$.

IV. Preliminary Sea Ice Retrieval Results

For the NT algorithm, sea ice retrievals from WindSat are closely correlated with those from SSM/I, with correlation coefficient of 0.962 and an offset of 5.4% ice concentration over-estimated by WindSat. However, the NT algorithm under-estimates ice concentrations at both high end [16] and and low end [17]. The NT2 algorithm was developed to

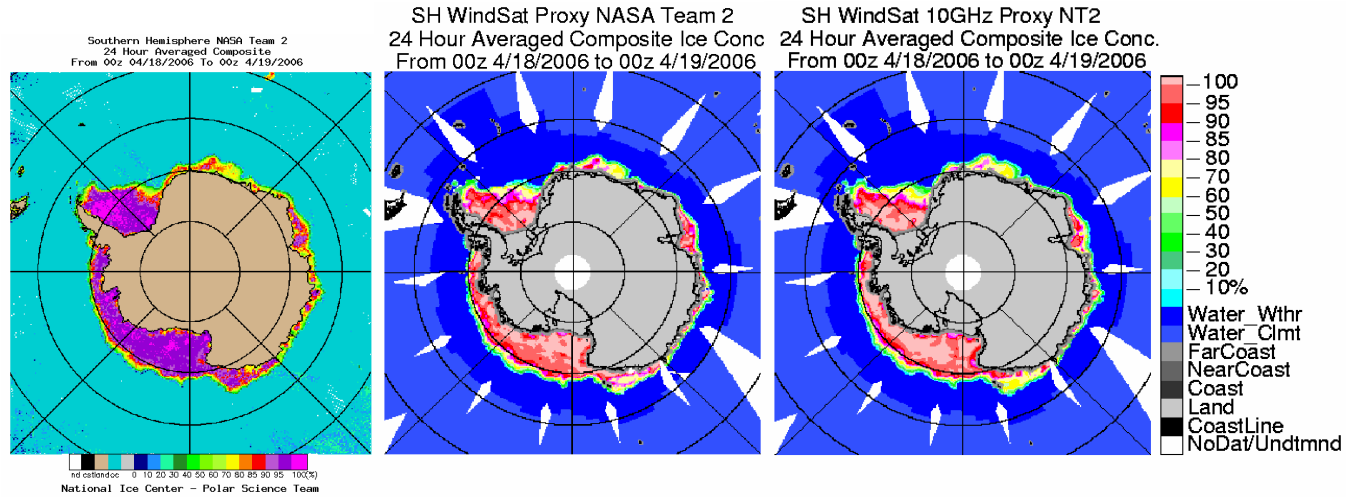

Fig. 6. Comparison of sea ice maps retrieved from SSM/I by NT2 algorithm and from WindSat by proxy NT2 and 10 GHz proxy NT2 algorithms. Note that in the WindSat maps, 'Water_Wthr" denotes the open water areas derived from the WindSat weather filter sets in the possible sea ice region, "Water_Clmt" denotes climatologically ice free areas, and "FarCoast" is defined as land contamination value 1 to 20%, "NearCoast" 21-40%, "Coast" 41-60%, and "Land" 61-100%.

correct snow-layered high concentrations [6]. A comparison of sea ice maps from SSM/I daily nowcast [9] by NT2 and WindSat near-real-time retrievals by proxy NT2 algorithms is shown in Fig. 6. The WindSat Proxy NT2 algorithms work compatibly well with SSM/I NT2 algorithms.

V. Concluding Remarks

This paper demonstrates that WindSat data can be used to successfully retrieve sea ice concentrations. Monthly sea ice climatology and modified weather filter sets reduce the sporadic false sea ice retrievals in open waters. Quantified land contamination flags false sea ice retrievals in the far- and near-coastal areas. Sea ice retrieved by WindSat modified NT algorithm compares well with SSM/I NT algorithm. Even without 85 GHz channels, WindSat proxy NT2 algorithms at 18.7 and 10.7 GHz are capable of retrieving snow-layered sea ice concentration. Validation of these algorithms with independent sea ice products from other instruments such as AVHRR and MODIS is ongoing.

Acknowledgement

This work is sponsored by the NPOESS Integrated Program Office. We thank the NRL WindSat team for providing the data.

References

[1] Peter W. Gaiser, et al., "The WindSat Spaceborne Polarimetric MicrowaveRadiometer: Sensor Description and Early Orbit Performance", *IEEE Trans. Geosci. Remote Sensing*, vol. 42, pp2347-2361. Nov. 2004.

[2] Carsey, Frank D. Ed., *Microwave Remote Sensing of Sea Ice*, Geophysical Monograph 68. American Geophysical Union, Washington, DC, 1992

[3] Bertoia, C., J. Falking ham, and F. Fetterer, "Polar SAR data for operational sea ice mapping," in *Analysis of SAR Data of Polar Oceans*, C. Tsatsoulis and R. Kwok, Eds, Berlin, Germany: Springer-Verlag, 1998.

[4] Schiermeier, Quirin, "A Sea Change", *NATURE*, Vol 439, pp256-260, 2006.

[5] Cavalieri, D.J., P. Gloersen, and W.J. Campbell, "Determination of sea ice parameters with the NIMBUS 7 scanning multichannel microwave radiometer," *J. Geophys. Res.*, vol. 89, pp. 5355–5369, 1984.

[6] Markus, T. and D.J. Cavalieri, "An Enhancement of the NASA Team Sea Ice Algorithm", *IEEE Trans. Geosci. Remote Sensing*, vol. 38, pp1387-1398, 2000.

[7] Comiso, J. 1990, updated current year. *DMSP SSM/I daily polar gridded sea ice concentrations*, June to September 2001. Edited by J. Maslanik and J. Stroeve. Boulder, CO: National Snow and Ice Data Center. Digital media.

[8] Cavalieri, D., P. Gloerson, and J. Zwally. 1990, updated current year. *DMSP SSM/I daily polar gridded sea ice concentrations*, June to September 2001. Edited by J. Maslanik and J. Stroeve. Boulder, CO: National Snow and Ice Data Center. Digital media.

[9] National Ice Center – Polar Science Team. http://science.natice.noaa.gov/products.htm.

[10] Grody, N.C., "Surface Identification Using Satellite Microwave Radiometers", *IEEE Trans. Geosci. Remote Sensing*, vol. 26, pp850-859, 1988.

[11] Hansen, M., R. DeFries, J.R.G. Townshend, and R. Sohlberg, "Global land cover classification at 1km resolution using a decision tree classifier", *Int'l J. Remote Sensing*. v. 21, pp: 1331-1365, 2000. Data online: http://glcf.umiacs.umd.edu/data/landcover.

[12] Loveland, T.R., B.C. Reed, J.F. Brown, D.O. Ohlen, J. Zhu, L. Yang, and J.W. Merchant, "Development of a Global Land Cover Characteristics Database and IGBP DISCover from 1-km AVHRR Data", *International J. Remote Sensing* , v. 21, p. 1303-1330, 2000. Data online: http://edcdaac.usgs.gov/glcc/globdoc2_0.asp.

[13] Gloersen, P. and D.J. Cavalieri, "Reduction of Weather Effects in the Calculation of Sea Ice concentration from Microwave Radiometers," *J. Geophys. Res.*, vol. 91, pp. 3913-3919, 1986.

[14] Cavalieri, D.J., K.M.St. Germain, and C.T. Swift, "Reduction of weather effects in the calculation of sea ice concentration with the DMSP SSM/I". J. *Glaciol.* 41(139):455-464, 1995.

[15] Pratt, William K., *Digital Imaging Processing*, 3rd Edition, John Wiley & Sons, Inc., New York, 2001.

[16] Comiso, J.C., D.J. Cavalieri, C.P. Parkinson, and P. Gloersen, "Passive microwave algorithms for sea ice concentration—A comparison of two techniques," *Remote Sens. Environ.*, vol. 60, pp. 357–384,1997.

[17] Cavalieri,*D.J.,* "A microwave technique for mapping thin sea-ice", *J. Geophys. Res.,* vol. 99, pp12561-12572, 1994.